8 Caturelli E, Castellano L, Fusilli S *et al.* Coarse nodular US pattern in hepatic cirrhosis: risk for hepatocellular carcinoma. *Radiology* 2003; **226**: 691–7.
9 Shimizu K, Katoh H, Yamashita F *et al.* Comparison of carbohydrate structures of serum α-fetoprotein by sequential glycosidase digestion and lectin affinity electrophoresis. *Clin. Chim. Acta* 1996; **254**: 23–40.
10 Mita Y, Aoyagi Y, Yanagi M, Suda T, Suzuki Y, Asakura H. The usefulness of determining des-gamma-carboxy prothrombin by sensitive enzyme immunoassay in the early diagnosis of patients with hepatocellular carcinoma. *Cancer* 1998; **82**: 1643–8.
11 Makuuchi M, Kokudo N, Arii S *et al.* Development of evidence-based clinical guidelines for the diagnosis and treatment of hepatocellular carcinoma in Japan. *Hepatol. Res.* 2008; **38**: 37–51.
12 Kudo M. Imaging diagnosis of hepatocellular carcinoma and premalignant/borderline lesions. *Semin. Liver Dis.* 1999; **19**: 297–309.
13 Torzilli G, Minagawa M, Takayama T *et al.* Accurate preoperative evaluation of liver mass lesions without fine-needle biopsy. *Hepatology* 1999; **30**: 889–93.
14 Vauthey JN, Lauwers GY, Esnaola NF *et al.* Simplified staging for hepatocellular carcinoma. *J. Clin. Oncol.* 2002; **20**: 1527–36.
15 Kaplan EL, Meier P. Non parametric estimation for incomplete observation. *J. Am. Stat. Assoc.* 1958; **53**: 457–81.
16 Petro R, Pike MC. Conservation of the approximation (0-E2)/E in the log rank test for survival data on tumor incidence data. *Biometrics* 1973; **29**: 579–84.
17 Pugh RNH, Murray-Lyon IM, Dawson JL *et al.* Transection of the oesophagus for bleeding oesophageal varices. *Br. J. Surg.* 1973; **60**: 646–9.
18 Miki D, Aikata H, Uka K *et al.* Clinicopathological features of elderly patients with hepatitis C virus related hepatocellular carcinoma. *J. Gastroenterol.* 2008; **43**: 550–7.
19 Saneto H, Kobayashi M, Kawamura Y *et al.* Clinicopathological features, background liver disease, and survival analysis of HCV-positive patients with hepatocellular carcinoma: differences between young and elderly patients. *J. Gastroenterol.* 2008; **43**: 975–81.
20 Kumada T, Toyoda H, Kiriyama S *et al.* Relation between incidence of hepatic carcinogenesis and integration value of alanine aminotransferase in patients with hepatitis C virus infection. *Gut* 2007; **56**: 738–9.
21 Kumada T, Toyoda H, Kiriyama S *et al.* Incidence of hepatocellular carcinoma in hepatitis C carriers with normal alanine aminotransferase levels. *J. Hepatol.* 2009; **50**: 729–35.
22 Oka H, Kurioka N, Kim K *et al.* Prospective study of early detection of hepatocellular carcinoma in patients with cirrhosis. *Hepatology* 1990; **12**: 680–7.
23 Ikeda K, Saitoh S, Koida I *et al.* A multivariate analysis of risk factors for hepatocellular carcinogenesis: a prospective observation of 795 patients with viral and alcoholic cirrhosis. *Hepatology* 1993; **18**: 47–53.
24 Hamada H, Yatsuhashi H, Yano K *et al.* Impact of aging on the development of hepatocellular carcinoma in patients with posttransfusion chronic hepatitis C. *Cancer* 2002; **95**: 331–9.
25 Yatsuhashi H, Yano M. Towards control of hepatitis C in the Asia-Pacific region. *J. Gastroenterol. Hepatol.* 2000; **15** (Suppl.): E111–16.
26 Chu CW, Hwang SJ, Luo JC *et al.* Clinical, virologic, and pathologic significance of elevated serum alpha-fetoprotein levels in patients with chronic hepatitis C. *J. Clin. Gastroenterol.* 2001; **32**: 240–4.
27 Balducci L, Extermann M. Management of cancer in the older person: a practical approach. *Oncologist* 2000; **5**: 224–37.
28 Goukassian D, Gad F, Yaar M, Eller MS, Nehal US, Gilchrest BA. Mechanisms and implications of the age-associated decrease in DNA repair capacity. *FASEB J.* 2000; **14**: 1325–34.
29 Lu SN, Wang JH, Liu SL *et al.* Thrombocytopenia as a surrogate for cirrhosis and a marker for the identification of patients at high-risk for hepatocellular carcinoma. *Cancer* 2006; **107**: 2212–22.

Journal of Medical Virology 85:228–234 (2013)

Comparison of the Efficacy of Ribavirin Plus Peginterferon Alfa-2b for Chronic Hepatitis C Infection in Patients With and Without Coagulation Disorders

Takashi Honda,[1] Yoshiaki Katano,[1]* Teiji Kuzuya,[1] Kazuhiko Hayashi,[1] Masatoshi Ishigami,[1] Akihiro Itoh,[1] Yoshiki Hirooka,[1] Isao Nakano,[1] Tetsuya Ishikawa,[1] Hidenori Toyoda,[2] Takashi Kumada,[2] Koji Yamamoto,[3] Tadashi Matsushita,[3] Tetsuhito Kojima,[3] Junki Takamatsu,[4] and Hidemi Goto[1]

[1]*Department of Gastroenterology and Hepatology, Nagoya University Graduate School of Medicine, Nagoya, Japan*
[2]*Department of Gastroenterology, Ogaki Municipal Hospital, Ogaki, Gifu, Japan*
[3]*Department of Transfusion Medicine, Nagoya University Hospital, Nagoya, Japan*
[4]*Aichi Blood Center Japanese Red Cross, Seto, Japan*

Many patients with coagulation disorders are infected with hepatitis C virus (HCV) that advances to end stage liver disease, resulting in an increased number of deaths. The efficacy of ribavirin and peginterferon combination therapy for chronic HCV infection in patients with coagulation disorders has not been clarified fully. The aim of this study was to evaluate the efficacy and tolerability of combination therapy in this patient population compared with patients who are infected with HCV and do not have coagulation disorders. A total of 226 consecutive chronic hepatitis C patients were treated with combination therapy and divided into two groups: patients with (n = 23) and without coagulation disorders (n = 203). Clinical characteristics, sustained virological response rates obtained by an intention-to-treat analysis, and combination therapy discontinuation rates were compared between the two groups. The sustained virological response rates did not differ significantly between patients with and without coagulation disorders (65.2% vs. 47.8% by intention-to-treat analysis). According to a multivariate analysis, age, alanine aminotransferase, gamma-glutamyltransferase, and HCV genotype were associated significantly with a sustained virological response, whereas whether a patient had a coagulation disorder did not affect the sustained virological response. In conclusion, combination therapy for chronic hepatitis C was comparably effective between patients with and without coagulation disorders and did not result in adverse bleeding. ***J. Med. Virol. 85:228–234, 2013.*** © 2012 Wiley Periodicals, Inc.

KEY WORDS: chronic hepatitis C; interferon; ribavirin; coagulation disorders; hemophilia

INTRODUCTION

Hepatitis C virus (HCV) infection is a widespread viral infection that often leads to chronic hepatitis, cirrhosis, and hepatocellular carcinoma. Until the 1980s, most patients with coagulation disorders became infected with HCV because of the extensive use of untreated factor concentrate. Some of these patients were infected with both hepatitis C and human immunodeficiency virus (HIV) [Brettler et al., 1990; Troisi et al., 1993; Yee et al., 2000; Franchini et al., 2001]. These patients with liver diseases and persistent abnormal transaminase progress to end stage liver disease, resulting in an increased number of liver disease-related deaths. In cases of co-infection with the HIV, the progression of liver disease is more rapid [Sanchez-Quijano et al., 1995; Soto et al., 1997; Benhamou et al., 1999; Ragni and Belle, 2001; De Luca et al., 2002] with a higher mortality rate than

Grant sponsor: Health Sciences Research Grants from the Ministry of Health, Labour and Welfare of Japan.

*Correspondence to: Yoshiaki Katano, Department of Gastroenterology and Hepatology, Nagoya University Graduate School of Medicine, 65 Tsuruma-Cho, Showa-Ku, Nagoya 466-8550, Japan E-mail: ykatano@med.nagoya-u.ac.jp

Accepted 10 September 2012

DOI 10.1002/jmv.23444

Published online 14 November 2012 in Wiley Online Library (wileyonlinelibrary.com).

during HCV monoinfection [Darby et al., 1997; Yee et al., 2000]. The need for treating infection with HCV in patients with coagulation disorders is increasing worldwide.

Sustained virological responders who are negative for serum HCV RNA 6 months after the end of treatment with interferon (IFN) are likely to remain in virological and biochemical remission with histologic improvement [Marcellin et al., 1997; Shiratori et al., 2000]. In addition, IFN therapy reduces the risk of hepatocellular carcinoma among virological or biochemical responders [Imai et al., 1998; Ikeda et al., 1999; Yoshida et al., 1999]. Ribavirin is now used generally in combination with IFN or pegIFN to treat chronic hepatitis C and combination therapy is more effective than IFN monotherapy [Lai et al., 1996; McHutchison et al., 1998; Poynard et al., 1998; Manns et al., 2001].

Previous studies have investigated the efficacy of IFN monotherapy in patients with coagulation disorders and chronic hepatitis C [Makris et al., 1991], and the efficacy of combination therapy with ribavirin and PegIFN in patients with coagulation disorders [Fried et al., 2002a; Mancuso et al., 2006; Posthouwer et al., 2007]. However, there are no reported comparisons of this combination therapy between patients infected with HCV with and without coagulation disorders. In this study, the efficacy and tolerability of ribavirin plus pegIFN were evaluated retrospectively in patients with coagulation disorders and chronic hepatitis C and the results were compared with the responses of patients infected with HCV but without coagulation disorders.

MATERIALS AND METHODS

Patients and Methods

A total of 226 consecutive patients with chronic hepatitis C and a high viral load (serum HCV RNA levels greater than 100 kilo-international units [KIU]) were treated with a combination of pegIFN and ribavirin between December 2004 and March 2007 at Nagoya University Hospital and Ogaki Municipal Hospital. These patients included 23 patients with coagulation disorders (17 with hemophilia A, 4 with hemophilia B, and 2 with von Willebrand disease). All patients were under 75 years old, were anti-HCV antibody-positive, and had serum HCV RNA levels greater than 100 KIU/ml by quantitative PCR assay (Amplicor GT-HCV Monitor Version 2.0; Roche Molecular Systems, Pleasanton, CA) within 12 weeks preceding the therapeutic period. Patients were excluded if they had pretreatment hemoglobin (Hb) levels <10 g/dl, tested positive for serum hepatitis B surface antigen, a history of drug addiction, alcohol abuse, autoimmune hepatitis, primary biliary cirrhosis, a serious psychiatric or medical illness, or were pregnant. To exclude patient bias, only complete cohorts from each hospital were enrolled. HCV genotypes were determined by PCR using genotype-specific primers [Okamoto et al., 1994; Simmonds et al., 1994].

All patients were treated with 1.5 μg/kg of pegIFN α-2b (Peg-Intron®, MSD, Tokyo, Japan) once weekly for 24 weeks in patients infected with HCV genotype 2 or 3 and for 48 weeks in patients infected with HCV genotype 1 or 4. For the 17 patients infected with HCV genotype 1, the treatment duration was extended to 72 weeks because of higher efficacy compared to that obtained after 48 weeks of treatment, but only in cases in which HCV RNA was positive at 12 weeks and negative at 24 weeks from the start of therapy. Treatment was discontinued when a patient's Hb concentration fell below 8.5 g/dl because of drug-induced hemolytic anemia or when a patient's white blood cell count fell below 1,000/mm^3, neutrophil count fell below 500/mm^3, or platelet count fell below 50,000/mm^3. Some patients discontinued treatment because the virus could not be eradicated after 24 weeks, as determined by the physician. The pegIFN alfa-2b dose was reduced to 50% of the assigned dose when the white blood cell count was below 1,500/mm^3, the neutrophil count below 750/mm^3 or the platelet count below 8,000/mm^3. Oral ribavirin (Rebetol®, MSD, Tokyo, Japan) was administered for the same duration as pegIFN at 600 mg/day for patients who weighed 60 kg or less, 800 mg/day for those who weighed more than 60 kg but less than 80 kg, and 1,000 mg/day for those who weighed more than 80 kg during the treatment period. The ribavirin dose was reduced by 200 mg/day when the patient's Hb concentration fell below 10 g/dl because of drug-associated hemolytic anemia. Ribavirin was discontinued when pegIFN therapy was discontinued. Informed consent was obtained from each patient and the study was performed in accordance with the 1975 Declaration of Helsinki.

Liver Histology

Pretreatment liver biopsy specimens were classified based on a fibrosis scale of F0 to F4 (F0, no fibrosis; F1, portal fibrosis without septa; F2, few septa; F3, numerous septa without cirrhosis; and F4, cirrhosis) and in terms of necroinflammatory activity on a scale of A0 to A3 (A0, no histological activity; A1, mild activity; A2, moderate activity; and A3, severe activity) [Bedossa and Poynard, 1996; Fried et al., 2002b]. In patients with coagulation disorders, a liver biopsy was performed using factor concentrate, provided the patients gave informed consent.

Assessment of Efficacy

The virological response was assessed by a qualitative HCV RNA assay with a lower sensitivity limit of 100 copies/ml (Amplicor HCV version 2.0; Roche Molecular Systems). According to the qualitative HCV RNA results, responses were defined as a sustained virological response if no HCV RNA was detected at the end of the 24-week follow-up period after the treatment was completed. A patient was considered to have an end of treatment virological response if no HCV RNA was detected at the end of treatment.

Comparison of Characteristics and Treatment Efficacy Between Patients With and Without Coagulation Disorders

Sex ratio, age, body weight, body mass index (BMI), baseline serum alanine aminotransferase (ALT) levels, gamma-glutamyltransferase (GGT), pretreatment Hb level, platelet counts, HCV genotype and viral load, histologic activity, and fibrosis were compared between patients with and without coagulation disorders. The sustained virological response rates obtained by an intention-to-treat analysis and per-protocol analysis, ribavirin and pegIFN dose reduction rates, and combination therapy discontinuation rates were compared between the two groups. The end of treatment virological response rate was obtained by intention-to-treat and per-protocol analyses and then compared between the two groups. Next, the variable accession method in a multivariate analysis was used to examine factors associated with a sustained virological response after combination therapy, including the following factors: sex, age, BMI, baseline serum ALT, GGT, platelet counts, genotype, HCV RNA concentration, and presence of a coagulation disorder.

Because efficacy differed by the HCV genotype and the patient age, and since all coagulation disorder patients were male, the analysis focused on male, age-matched patients infected with HCV genotype 1. The characteristics and efficacy of treatment were compared in males, and age-matched patients with and without coagulation disorders who were infected with HCV-genotype 1.

Statistical Analysis

Values are expressed as the means ± SDs. Between-group differences in mean quantitative values were analyzed by Student's *t*-test, and differences in nonparametric data were analyzed by the Mann–Whitney *U*-test. Differences in proportions were examined by the Chi-squared test. Multiple logistic regression analysis was used to identify factors related to a sustained virological response. All statistical analyses were performed using SAS software (SAS Institute, Cary, NC). All P values were two-tailed, and $P < 0.05$ was considered statistically significant.

RESULTS

Patient Characteristics

The patients included 127 men and 99 women aged 22–74 years (mean ± SD, 54.7 ± 11.6). The mean age of patients without coagulation disorders was 56.3 ± 10.9 years and most patients were in their 50s and 60s. In contrast, the mean age of patients with coagulation disorders was 41.5 ± 9.8 years with an age distribution ranging from 20 to 50 years. The clinical characteristics of the two study groups are shown in Table I. All patients with coagulation disorders in this study were male because of inherited, sex-linked hemophilia, and two patients in this study had male von Willebrand disease. Patients with coagulation disorders were significantly younger than patients without coagulation disorders ($P < 0.0001$). Although body weight was not different between the two groups, patients with coagulation disorders had a significantly lower BMI than patients without coagulation disorders. Patients without coagulation disorders were infected with HCV genotypes that are not unique to Japan, such as genotypes 1a, 3a, and 4a. Four patients with coagulation disorders were infected with human immunodeficiency virus and one of these patients had achieved a sustained virological response.

Response to Therapy

The ribavirin dose reduction rate tended to be higher in patients without coagulation disorders than in patients with coagulation disorders ($P = 0.0643$). The treatment discontinuation rate did not differ significantly between the two groups. As a result, the sustained virological response rate by an intention-to-treat analysis did not differ significantly between the

TABLE I. Clinical Characteristics of Patients Treated With Combination Therapy

	Total patients (n = 226)	Patients without coagulation disorders (n = 203)	Patients with coagulation disorders (n = 23)	*P* value
Sex ratio (male/female)	127/99	104/99	23/0	<0.0001
Age (years)	54.7 ± 11.6	56.3 ± 10.9	41.5 ± 9.8	<0.0001
Body weight (kg)	60.2 ± 11.1	60.5 ± 11.5	60.5 ± 8.1	0.9972
Body mass index	22.9 ± 3.1	23.1 ± 3.1	21.5 ± 2.5	0.0226
Baseline serum ALT (IU/L)	63.3 ± 56.8	60.9 ± 54.9	84.4 ± 69.1	0.0598
GGT (IU/L)	54.2 ± 63.9	51.4 ± 62.2	78.6 ± 74.4	0.0526
Hemoglobin (g/dl)	14.1 ± 1.3	14.1 ± 1.3	14.4 ± 1.3	0.2714
Platelets ($\times 10^4/\mu l$)	17.8 ± 5.2	17.7 ± 5.2	19.0 ± 5.6	0.2597
Genotype (1a/1b/2a/2b/3a/4a)	7/160/40/15/3/1	0/150/39/14/0/0	7/10/1/1/3/1	<0.0001
HCV RNA (KIU/ml)	1,898.0 ± 1,448.3	1,923.1 ± 1,464.5	1,676.6 ± 1,305.1	0.4404
Activity (A0/A1/A2/A3)	2/108/71/11	2/101/64/11	0/7/7/0	0.3442
Fibrosis (F0/F1/F2/F3)	17/104/49/22	16/97/45/20	1/7/4/2	0.5351

ALT, alanine aminotransferase; GGT, gamma-glutamyltransferase; HCV RNA, hepatitis C virus RNA; KIU, kilo-international units.

TABLE II. Efficacy of Combination Therapy

	Total patients (n = 226)	Patients without coagulation disorders (n = 203)	Patients with coagulation disorders (n = 23)	*P* value
SVR rate (intention-to-treat)	49.6 (112/226)	47.8 (97/203)	65.2 (15/23)	0.1130
SVR rate (per-protocol)	54.4 (111/204)	52.7 (97/184)	70.0 (14/20)	0.1405
ETR rate (intention-to-treat)	84.1 (190/226)	84.7 (172/203)	78.3(18/23)	0.4218
ETR rate (per-protocol)	89.1 (179/201)	89.6 (163/182)	84.2 (16/19)	0.4772
Ribavirin dose reduction rate	44.2 (100/226)	46.3 (94/203)	26.1 (6/23)	0.0643
PegIFN dose reduction rate	34.1 (77/226)	33.5 (68/203)	39.1 (9/23)	0.5891
Combination therapy discontinuation rate	9.8 (22/226)	9.4 (19/203)	13.0 (3/23)	0.5722

SVR, sustained virological response; ETR, end of treatment virological response; PegIFN, peginterferon.

two groups. The sustained virological response rate of patients with coagulation disorders by a per-protocol analysis was higher than that of patients without coagulation disorders, but there was no significant difference. In addition, based on both intention-to-treat and per-protocol analyses, the end of treatment virological response rate did not differ significantly between the two groups (Table II).

Factors associated with a sustained virological response in combination therapy were determined by a multivariate analysis. HCV genotype 1 and 4 versus 2 and 3 ($P = 0.001$, odds ratio 4.353 [95% CI, 1.810–10.469]), baseline serum GGT ($P = 0.003$, odds ratio 1.018 [1.006–1.030]), age ($P = 0.006$, odds ratio 1.053 [1.015–1.093]), and baseline serum ALT ($P = 0.014$, odds ratio 0.991 [0.983–0.998]) were associated significantly with a sustained virological response, but whether or not a patient had a coagulation disorder was not associated significantly with a sustained virological response.

Characteristics and Response of Male, Age-Matched Patients Infected With HCV Genotype 1

The clinical characteristics of the two study groups in the male, age-matched patients infected with HCV genotype 1 are shown in Table III. Body weight, BMI, and Hb levels were significantly lower in patients with coagulation disorders than patients without coagulation disorders ($P = 0.0003$, 0.0027, and 0.0103, respectively).

The treatment discontinuation rate of patients with coagulation disorders did not differ between the two groups. The sustained virological response rate by intention-to-treat and per-protocol analyses did not differ significantly between the two groups (Table IV). Factors associated with a sustained virological response in the male, age-matched, genotype 1 patients treated with combination therapy were determined by a multivariate analysis. BMI ($P = 0.036$, odds ratio 1.810 [1.041–3.145]) and baseline serum GGT ($P = 0.037$, odds ratio 0.981 [0.963–0.999]) were associated significantly with a sustained virological response, but whether or not a patient had a coagulation disorder was not associated significantly with a sustained virological response.

Adverse Events

The reasons for discontinuing combination therapy and the times at which the therapy was discontinued are shown in Table V. Once treatment was discontinued, therapy was not restarted even after the initial symptoms or illness disappeared. There were no bleeding episodes in the patients with coagulation disorders, including patients who received a liver biopsy.

TABLE III. Clinical Characteristics of Male, Age-Matched Patients With Genotype 1 Treated With Combination Therapy

	Total patients (n = 36)	Patients without coagulation disorders (n = 18)	Patients with coagulation disorders (n = 18)	*P* value
Age (years)	42.8 ± 8.0	44.9 ± 5.9	40.7 ± 9.3	0.1136
Body weight (kg)	66.1 ± 11.0	73.4 ± 9.3	60.4 ± 8.7	0.0003
Body mass index	22.7 ± 2.8	24.3 ± 2.3	21.4 ± 2.5	0.0027
Baseline serum ALT (IU/L)	69.8 ± 54.3	63.5 ± 31.7	76.2 ± 70.5	0.4919
GGT (IU/L)	72.7 ± 64.2	74.3 ± 71.1	71.2 ± 58.5	0.8869
Hemoglobin (g/dl)	14.9 ± 1.2	15.4 ± 1.0	14.4 ± 1.2	0.0103
Platelets ($\times 10^4/\mu l$)	19.3 ± 5.4	18.8 ± 4.5	19.8 ± 5.6	0.5773
HCV RNA (KIU/ml)	2,050.8 ± 1,273.4	2,322.8 ± 1,249.1	1,778.8 ± 1,273.5	0.2044
Activity (A0/A1/A2/A3)	0/12/11/0	0/6/5/0	0/6/6/0	0.6723
Fibrosis (F0/F1/F2/F3)	2/11/8/2	1/5/4/1	1/6/4/1	0.9392

ALT, alanine aminotransferase; GGT, gamma-glutamyltransferase; HCV RNA, hepatitis C virus RNA; KIU, kilo-international unit.

TABLE IV. Efficacy of Combination Therapy in Male, Age-Matched Patients With Genotype 1

	Total patients (n = 36)	Patients without coagulation disorders (n = 18)	Patients with coagulation disorders (n = 18)	*P* value
SVR rate (intention-to-treat)	58.3 (21/36)	61.1 (11/18)	55.6 (10/18)	0.7353
SVR rate (per-protocol)	69.0 (20/29)	64.7 (11/17)	75.0 (9/12)	0.5551
ETR rate (intention-to-treat)	77.8 (28/36)	83.3 (15/18)	72.2 (13/18)	0.4227
ETR rate (per-protocol)	93.1 (27/29)	88.2 (15/17)	100.0 (12/12)	0.2182
Ribavirin dose reduction rate	22.2 (28/36)	16.7 (3/18)	27.8 (5/18)	0.7175
PegIFN dose reduction rate	36.1 (13/36)	27.8 (5/18)	44.4 (8/18)	0.2979
Combination therapy discontinuation rate	5.6 (2/36)	0 (0/18)	16.7 (3/18)	0.0704

SVR, sustained virological response; ETR, end of treatment virological response; PegIFN, peginterferon.

DISCUSSION

A previous randomized trial in patients infected with HCV with inherited bleeding disorders showed that the sustained virological response rate improved significantly for patients who were treated with IFN and ribavirin compared to those treated with IFN alone [Fried et al., 2002a]. In addition, both chronic hepatitis C patients with and without coagulation disorders responded similarly to pegIFN and ribavirin combination therapy [Franchini et al., 2006; Posthouwer et al., 2006]. However, the efficacy and tolerability of this combination therapy differed based on the HCV genotype as well as the age, gender, and race of the patients; therefore it is difficult to compare patients with and without coagulation disorders under the same conditions. No report has examined that patients infected chronic hepatitis C with and without coagulation disorders at the same institution and during the same observation period. In addition, there are no reports on the efficacy of combination therapy in patients with chronic hepatitis C with and without coagulation disorders in age-matched patients infected with HCV genotype 1. Therefore, a retrospective study was conducted to evaluate the efficacy and tolerability of ribavirin plus pegIFN in chronic hepatitis C patients with and without coagulation disorders. In the per-protocol analysis, there were no significant differences, but the sustained virological response rate was higher in patients with coagulation disorders than in patients without coagulation disorders. Mancuso et al. [2006] reported that combination therapy with pegIFN alfa-2b plus ribavirin is highly efficacious in hemophiliacs with chronic hepatitis C. In an overall analysis, patients with coagulation disorders had a lower mean age than patients without coagulation disorders. In addition, the BMI of the patients with coagulation disorders was lower than that of patients without coagulation disorders. A multivariate analysis showed that the HCV genotype, baseline serum GGT, age, and baseline ALT were factors associated significantly with a sustained virological response and whether patients had coagulation disorders was not associated with a sustained virological response. Age, especially younger than 40 years old, was a good predictive factor for a sustained virological response, as was reported previously [Poynard et al., 2000; Fried et al., 2002b].

TABLE V. Reasons for Discontinuing Combination Therapy

Reason	Number	Weeks after starting treatment
Patients with coagulation disorders		
Peritonitis due to appendicitis	1	16
Pneumoniae	1	18
No HCV eradication	3	24, 28, 29
IDDM	1	44
Patients without coagulation disorders		
Fatigue	5	1, 2, 4.9, 19
Bleeding from duodenal varies	1	8
Dizziness	1	12
Palpitation	1	13
Cholecystitis	1	16
Symptom of Parkinson's disease	1	16
Fundal hemorrhage	1	17
Hepatocellular carcinoma	2	19, 21
Suspicion of Interstitial pneumonia	1	20
Gastric cancer	2	21, 36
Self-discontinuation	1	24
Neutropenia	1	25
Eruption	1	25
No HCV eradication	7	24, 25, 25, 27, 28, 29, 29

These results suggest that male patients who are infected with HCV genotype 1 and have coagulation disorders will have a higher sustained virological response than patients without coagulation disorders, if the coagulation disorder patients do not discontinue treatment. However, these results do not account for the differences in age. Therefore, male, age-matched patients infected with HCV genotype 1 were evaluated. The characteristics that differed between patients with and without coagulation disorders were body weight, BMI and baseline Hb levels.

In male, age-matched patients infected with HCV genotype 1, the sustained virological response rate based on both intention-to-treat and per-protocol analyses was not different between patients with and without coagulation disorders.

Using a multivariate analysis, whether patients had coagulation disorders was not associated significantly with a sustained virological response. Only BMI and GGT were identified as factors associated with a sustained virological response to combination therapy in male, age-matched patients infected with HCV genotype 1. A previous report showed that GGT levels may represent a surrogate marker of tumor necrosis factor-alpha expression in the liver and explain the importance of serum analyses to in predict the treatment outcome [Taliani et al., 2002]. Several studies revealed that GGT is one predictor of a sustained virological response [Taliani et al., 2002, 2006; Villela-Nogueira et al., 2005]. In western countries, obesity and a high BMI are associated with the absence of a sustained virological response to combination therapy of pegIFN or IFN with ribavirin [Bressler et al., 2003; Camma et al., 2004]. However, in Japan, most of the patients who are treated with combination therapy are not obese and have lower BMIs than patients in western countries. In this population, the mean BMI was 22.7 $\pm$ 2.8. In this low BMI population, a higher BMI would be associated with a sustained virological response. However, the reason why a low BMI is associated with the absence of a sustained virological response has not elucidated.

Adverse effects are thought to increase in patients with coagulation disorders; however, there was not a significant difference in adverse effects necessitating discontinuation of pegIFN and ribavirin between patients with and without coagulation disorders (13.0% vs. 9.4%). In addition, severe adverse effects and bleeding adverse effects were not associated with coagulation disorders. A previous report showed that IFN and ribavirin combination therapy may reduce the use of clotting factors in hemophilia patients with chronic hepatitis C [Honda et al., 2005; Yamamoto et al., 2006]. Ribavirin may reduce the side effect of bleeding during combination therapy. In this study, patients with coagulation disorders did not experience an adverse effect of bleeding.

In conclusion, treatment of chronic hepatitis C with combination therapy was effective comparably between patients with and without coagulation disorders and there were no adverse effects of bleeding.

REFERENCES

Bedossa P, Poynard T. 1996. An algorithm for the grading of activity in chronic hepatitis C. The METAVIR Cooperative Study Group. Hepatology 24:289–293.

Benhamou Y, Bochet M, Di Martino V, Charlotte F, Azria F, Coutellier A, Vidaud M, Bricaire F, Opolon P, Katlama C, Poynard T. 1999. Liver fibrosis progression in human immunodeficiency virus and hepatitis C virus coinfected patients. The Multivirc Group. Hepatology 30:1054–1058.

Bressler BL, Guindi M, Tomlinson G, Heathcote J. 2003. High body mass index is an independent risk factor for nonresponse to antiviral treatment in chronic hepatitis C. Hepatology 38:639–644.

Brettler DB, Alter HJ, Dienstag JL, Forsberg AD, Levine PH. 1990. Prevalence of hepatitis C virus antibody in a cohort of hemophilia patients. Blood 76:254–256.

Camma C, Di Bona D, Schepis F, Heathcote EJ, Zeuzem S, Pockros PJ, Marcellin P, Balart L, Alberti A, Craxi A. 2004. Effect of peginterferon alfa-2a on liver histology in chronic hepatitis C: A meta-analysis of individual patient data. Hepatology 39:333–342.

Darby SC, Ewart DW, Giangrande PL, Spooner RJ, Rizza CR, Dusheiko GM, Lee CA, Ludlam CA, Preston FE. 1997. Mortality from liver cancer and liver disease in haemophilic men and boys in UK given blood products contaminated with hepatitis C. UK Haemophilia Centre Directors' Organisation. Lancet 350:1425–1431.

De Luca A, Bugarini R, Lepri AC, Puoti M, Girardi E, Antinori A, Poggio A, Pagano G, Tositti G, Cadeo G, Macor A, Toti M, D'Arminio Monforte A. 2002. Coinfection with hepatitis viruses and outcome of initial antiretroviral regimens in previously naive HIV-infected subjects. Arch Intern Med 162:2125–2132.

Franchini M, Rossetti G, Tagliaferri A, Capra F, de Maria E, Pattacini C, Lippi G, Lo Cascio G, de Gironcoli M, Gandini G. 2001. The natural history of chronic hepatitis C in a cohort of HIV-negative Italian patients with hereditary bleeding disorders. Blood 98:1836–1841.

Franchini M, Nicolini N, Capra F. 2006. Treatment of hepatitis C in hemophiliacs. Am J Hematol 81:696–702.

Fried MW, Peter J, Hoots K, Gaglio PJ, Talbut D, Davis PC, Key NS, White GC, Lindblad L, Rickles FR, Abshire TC. 2002a. Hepatitis C in adults and adolescents with hemophilia: A randomized, controlled trial of interferon alfa-2b and ribavirin. Hepatology 36:967–972.

Fried MW, Shiffman ML, Reddy KR, Smith C, Marinos G, Goncales FL Jr, Haussinger D, Diago M, Carosi G, Dhumeaux D, Craxi A, Lin A, Hoffman J, Yu J. 2002b. Peginterferon alfa-2a plus ribavirin for chronic hepatitis C virus infection. N Engl J Med 347: 975–982.

Honda T, Toyoda H, Hayashi K, Katano Y, Yano M, Nakano I, Yoshioka K, Goto H, Yamamoto K, Takamatsu J. 2005. Ribavirin and use of clotting factors in patients with hemophilia and chronic hepatitis C. JAMA 293:1190–1192.

Ikeda K, Saitoh S, Arase Y, Chayama K, Suzuki Y, Kobayashi M, Tsubota A, Nakamura I, Murashima N, Kumada H, Kawanishi M. 1999. Effect of interferon therapy on hepatocellular carcinogenesis in patients with chronic hepatitis type C: A long-term observation study of 1,643 patients using statistical bias correction with proportional hazard analysis. Hepatology 29:1124–1130.

Imai Y, Kawata S, Tamura S, Yabuuchi I, Noda S, Inada M, Maeda Y, Shirai Y, Fukuzaki T, Kaji I, Ishikawa H, Matsuda Y, Nishikawa M, Seki K, Matsuzawa Y. 1998. Relation of interferon therapy and hepatocellular carcinoma in patients with chronic hepatitis C. Osaka Hepatocellular Carcinoma Prevention Study Group. Ann Intern Med 129:94–99.

Lai MY, Kao JH, Yang PM, Wang JT, Chen PJ, Chan KW, Chu JS, Chen DS. 1996. Long-term efficacy of ribavirin plus interferon alfa in the treatment of chronic hepatitis C. Gastroenterology 111:1307–1312.

Makris M, Preston FE, Triger DR, Underwood JC, Westlake L, Adelman MI. 1991. A randomized controlled trial of recombinant interferon-alpha in chronic hepatitis C in hemophiliacs. Blood 78:1672–1677.

Mancuso ME, Rumi MG, Santagostino E, Linari S, Coppola A, Mannucci PM, Colombo M. 2006. High efficacy of combined therapy

with pegylated interferon plus ribavirin in patients with hemophilia and chronic hepatitis C. Haematologica 91:1367–1371.

Manns MP, McHutchison JG, Gordon SC, Rustgi VK, Shiffman M, Reindollar R, Goodman ZD, Koury K, Ling M, Albrecht JK. 2001. Peginterferon alfa-2b plus ribavirin compared with interferon alfa-2b plus ribavirin for initial treatment of chronic hepatitis C: A randomised trial. Lancet 358:958–965.

Marcellin P, Boyer N, Gervais A, Martinot M, Pouteau M, Castelnau C, Kilani A, Areias J, Auperin A, Benhamou JP, Degott C, Erlinger S. 1997. Long-term histologic improvement and loss of detectable intrahepatic HCV RNA in patients with chronic hepatitis C and sustained response to interferon-alpha therapy. Ann Intern Med 127:875–881.

McHutchison JG, Gordon SC, Schiff ER, Shiffman ML, Lee WM, Rustgi VK, Goodman ZD, Ling MH, Cort S, Albrecht JK. 1998. Interferon alfa-2b alone or in combination with ribavirin as initial treatment for chronic hepatitis C. Hepatitis Interventional Therapy Group. N Engl J Med 339:1485–1492.

Okamoto H, Mishiro S, Tokita H, Tsuda F, Miyakawa Y, Mayumi M. 1994. Superinfection of chimpanzees carrying hepatitis C virus of genotype II/1b with that of genotype III/2a or I/1a. Hepatology 20:1131–1136.

Posthouwer D, Mauser-Bunschoten EP, Fischer K, Makris M. 2006. Treatment of chronic hepatitis C in patients with haemophilia: A review of the literature. Haemophilia 12:473–478.

Posthouwer D, Yee TT, Makris M, Fischer K, Griffioen A, Van Veen JJ, Mauser-Bunschoten EP. 2007. Antiviral therapy for chronic hepatitis C in patients with inherited bleeding disorders: An international, multicenter cohort study. J Thromb Haemost 5: 1624–1629.

Poynard T, Marcellin P, Lee SS, Niederau C, Minuk GS, Ideo G, Bain V, Heathcote J, Zeuzem S, Trepo C, Albrecht J. 1998. Randomised trial of interferon alpha2b plus ribavirin for 48 weeks or for 24 weeks versus interferon alpha2b plus placebo for 48 weeks for treatment of chronic infection with hepatitis C virus. International Hepatitis Interventional Therapy Group (IHIT). Lancet 352:1426–1432.

Poynard T, McHutchison J, Goodman Z, Ling MH, Albrecht J. 2000. Is an "a la carte" combination interferon alfa-2b plus ribavirin regimen possible for the first line treatment in patients with chronic hepatitis C? The ALGOVIRC Project Group. Hepatology 31:211–218.

Ragni MV, Belle SH. 2001. Impact of human immunodeficiency virus infection on progression to end-stage liver disease in individuals with hemophilia and hepatitis C virus infection. J Infect Dis 183:1112–1115.

Sanchez-Quijano A, Andreu J, Gavilan F, Luque F, Abad MA, Soto B, Munoz J, Aznar JM, Leal M, Lissen E. 1995. Influence of human immunodeficiency virus type 1 infection on the natural course of chronic parenterally acquired hepatitis C. Eur J Clin Microbiol Infect Dis 14:949–953.

Shiratori Y, Imazeki F, Moriyama M, Yano M, Arakawa Y, Yokosuka O, Kuroki T, Nishiguchi S, Sata M, Yamada G, Fujiyama S, Yoshida H, Omata M. 2000. Histologic improvement of fibrosis in patients with hepatitis C who have sustained response to interferon therapy. Ann Intern Med 132:517–524.

Simmonds P, Alberti A, Alter HJ, Bonino F, Bradley DW, Brechot C, Brouwer JT, Chan SW, Chayama K, Chen DS, Choo QL, Colombo M, Cuypers HM, Date T, Dusheiko GM, Esteban JI, Fay O, Hadziyannis SJ, Han J, Hatzakis A, Holmes EC, Hotta H, Houghton M, Irvine B, Kohara M, Kolberg JA, Kuo G, Lau JN, Lelie PN, Maertens G, McOmish F, Miyamura T, Mizokami M, Nomoto A, Prince AM, Reesink HW, Rice C, Roggendorf M, Schalm SW, Shikata T, Shimotohno K, Stuyver L, Trépo C, Weiner A, Yap PL, Urdea MS. 1994. A proposed system for the nomenclature of hepatitis C viral genotypes. Hepatology 19: 1321–1324.

Soto B, Sanchez-Quijano A, Rodrigo L, del Olmo JA, Garcia-Bengoechea M, Hernandez-Quero J, Rey C, Abad MA, Rodriguez M, Sales Gilabert M, Gonzalez F, Miron P, Caruz A, Relimpio F, Torronteras R, Leal M, Lissen E. 1997. Human immunodeficiency virus infection modifies the natural history of chronic parenterally-acquired hepatitis C with an unusually rapid progression to cirrhosis. J Hepatol 26:1–5.

Taliani G, Badolato MC, Nigro G, Biasin M, Boddi V, Pasquazzi C, Clerici M. 2002. Serum concentration of gammaGT is a surrogate marker of hepatic TNF-alpha mRNA expression in chronic hepatitis C. Clin Immunol 105:279–285.

Taliani G, Gemignani G, Ferrari C, Aceti A, Bartolozzi D, Blanc PL, Capanni M, Esperti F, Forte P, Guadagnino V, Mari T, Marino N, Milani S, Pasquazzi C, Rosina F, Tacconi D, Toti M, Zignego AL, Messerini L, Stroffolini T. 2006. Pegylated interferon alfa-2b plus ribavirin in the retreatment of interferon-ribavirin nonresponder patients. Gastroenterology 130:1098–1106.

Troisi CL, Hollinger FB, Hoots WK, Contant C, Gill J, Ragni M, Parmley R, Sexauer C, Gomperts E, Buchanan G, Schwartz B, Adair S, Fields H. 1993. A multicenter study of viral hepatitis in a United States hemophilic population. Blood 81:412–418.

Villela-Nogueira CA, Perez RM, de Segadas Soares JA, Coelho HS. 2005. Gamma-glutamyl transferase (GGT) as an independent predictive factor of sustained virologic response in patients with hepatitis C treated with interferon-alpha and ribavirin. J Clin Gastroenterol 39:728–730.

Yamamoto K, Honda T, Matsushita T, Kojima T, Takamatsu J. 2006. Anti-HCV agent, ribavirin, elevates the activity of clotting factor VII in patients with hemophilia: A possible mechanism of decreased events of bleeding in patients with hemophilia by ribavirin. J Thromb Haemost 4:469–470.

Yee TT, Griffioen A, Sabin CA, Dusheiko G, Lee CA. 2000. The natural history of HCV in a cohort of haemophilic patients infected between 1961 and 1985. Gut 47:845–851.

Yoshida H, Shiratori Y, Moriyama M, Arakawa Y, Ide T, Sata M, Inoue O, Yano M, Tanaka M, Fujiyama S, Nishiguchi S, Kuroki T, Imazeki F, Yokosuka O, Kinoyama S, Yamada G, Omata M. 1999. Interferon therapy reduces the risk for hepatocellular carcinoma: National surveillance program of cirrhotic and noncirrhotic patients with chronic hepatitis C in Japan. IHIT Study Group. Inhibition of Hepatocarcinogenesis by Interferon Therapy. Ann Intern Med 131:174–181.

Hypovascular Nodules in Patients with Chronic Liver Disease: Risk Factors for Development of Hypervascular Hepatocellular Carcinoma[1]

Tomoko Hyodo, MD
Takamichi Murakami, MD, PhD
Yasuharu Imai, MD, PhD
Masahiro Okada, MD, PhD
Masatoshi Hori, MD, PhD
Yuki Kagawa, MD, PhD
Sachiyo Kogita, MD
Seishi Kumano, MD, PhD
Masatoshi Kudo, MD, PhD
Teruhito Mochizuki, MD

Purpose: To identify patient characteristics and magnetic resonance (MR) imaging findings associated with subsequent hypervascularization in hypovascular nodules that show hypointensity on hepatobiliary phase gadoxetic acid–enhanced MR images in patients with chronic liver diseases.

Materials and Methods: Institutional review board approval was obtained, and informed consent was waived. At multiple follow-up gadoxetic acid–enhanced MR imaging examinations of 68 patients, 160 hypovascular nodules were retrospectively reviewed. A Cox regression model for hypervascularization was developed to explore the association of baseline characteristics, including patient factors (Child-Pugh classification, etiology of liver disease, history of local therapy for hepatocellular carcinoma [HCC], and coexistence of hypervascular HCC) and MR imaging findings (fat content, signal intensity on T2-weighted images, and nodule size). In addition, the growth rate was calculated as the reciprocal of tumor volume doubling time to investigate its relationship with subsequent hypervascularization by using receiver operating characteristic and Kaplan-Meier analyses.

Results: The prevalence of subsequent hypervascularization was 31% (50 of 160 nodules). Independent Cox multivariable predictors of increased risk of hypervascularization were hyperintensity on T2-weighted images (hazard ratio [HR] = 8.7; 95% confidence interval [CI]: 3.6, 20.8), previous local therapy for hypervascular HCC (HR = 5.0; 95% CI: 1.8, 13.6), Child-Pugh B cirrhosis (HR = 3.6; 95% CI: 1.4, 9.5) and coexistence of hypervascular HCC (HR = 2.0; 95% CI: 1.0, 3.8). The mean growth rate was significantly higher in nodules that showed subsequent hypervascularization than in those without hypervascularization. Kaplan-Meier analysis based on the receiver operating characteristic cutoff level (1.8×10^{-3}/day [tumor volume doubling time, 542 days]) showed that nodules with a higher growth rate had a significantly higher incidence of hypervascularization ($P = 5.2 \times 10^{-8}$, log-rank test).

Conclusion: Hyperintensity on T2-weighted images is an independent and strong risk factor at baseline for subsequent hypervascularization in hypovascular nodules in patients with chronic liver disease. Tumor volume doubling time of less than 542 days was associated with a high rate of subsequent hypervascularization.

[1] From the Departments of Radiology (T.H., T. Murakami, M.O., Y.K.) and Internal Medicine (M.K.), Kinki University Faculty of Medicine, 377-2 Ohno-Higashi, Osaka-Sayama, Osaka 589-8511, Japan; Department of Gastroenterology, Ikeda Municipal Hospital, Osaka, Japan (Y.I., S. Kogita); Department of Radiology, Osaka University Graduate School of Medicine, Suita, Japan (M.H.); Department of Radiology, Osaka Medical College, Takatsuki, Japan (S. Kumano); and Department of Diagnostic and Therapeutic Radiology, Ehime University Graduate School of Medicine, Toon, Japan (T.H., T. Mochizuki). From the 2011 RSNA Annual Meeting. Received December 16, 2011; revision requested January 30, 2012; revision received July 30; accepted August 29; final version accepted September 18. Supported by an Osaka Cancer Foundation grant. **Address correspondence to** T.H. (e-mail: *neneth@m.ehim-u.ac.jp*).

Follow-up surveillance of patients with cirrhosis has been performed to detect hepatocellular carcinoma (HCC) early enough to allow curative treatment (1). The American Association for the Study of Liver Diseases practice guidelines outline a strategy for distinguishing HCCs from other hepatic lesions of smaller than 3 cm that are identified during ultrasound (US) screening of livers in patients with cirrhosis (2). The guidelines suggest that nodules greater than 1 cm in diameter be further investigated by using dynamic contrast material–enhanced computed tomography (CT) or magnetic resonance (MR) imaging. Thus, the detection of arterial hypervascularization can justify treating the nodule as if it were HCC. For hypovascular nodules, defined as lesions that appear less enhanced than the surrounding liver both on arterial and venous phase images (2), careful monitoring (eg, repeat US at 3 months and biopsy) is recommended. However, the existing treatment guidelines do not specify the patient and tumor attributes that accurately predict subsequent hypervascularization.

Advances in Knowledge

- In patients with chronic liver disease, 31% (50 of 160) of the hypovascular nodules that showed hypointensity in the hepatobiliary phase of gadoxetic acid–enhanced MR imaging became hypervascular, which is a 1-year cumulative incidence of 25%.
- Hepatic hypovascular nodules that showed hyperintensity on T2-weighted images were at the highest risk for development of hypervascular hepatocellular carcinoma (hazard ratio, 8.7; 95% CI: 3.6, 20.8; $P < .001$).
- The higher growth rate (tumor volume doubling time, < 542 days) of a hepatic hypovascular nodule was associated with its subsequent development to hypervascular hepatocellular carcinoma.

The hepatobiliary phase of gadoxetic acid–enhanced MR imaging can allow clear visualization of hepatic focal lesions (3–6). Along with the widespread use of advanced imaging techniques, including three-dimensional T1-weighted gradient-echo sequences with high spatial resolution (7), hypovascular small nodules that show hypointensity on gadoxetic acid–enhanced hepatobiliary phase MR images are increasingly detected during HCC screening of patients with cirrhosis. Such nodules may include hypovascular well-differentiated HCCs, dysplastic nodules, and other benign nodules (8), which are difficult to distinguish, even at needle biopsy. Of these, hypovascular HCC and dysplastic nodules grow and acquire a more extensive arterial supply, and show overt stromal invasion (invasive growth of tumor tissue in portal tracts and fibrous septa), during stepwise carcinogenesis of HCC (9,10).

Previously, image-based studies suggested that hypovascular nodules containing fat or those that were greater than 10–15 mm in diameter were at high risk for development of hypervascularization (11–13). Authors of a histopathologic study (14) reported that most borderline nodules (dysplastic nodules or well-differentiated HCCs) greater than 15 mm in diameter were early HCC. Because these results were taken from findings at a single time point, further research examining the time course of the development of this change is required for the development of a better approach to follow-up of these hypovascular nodules.

Implications for Patient Care

- MR imaging findings may provide useful diagnostic information for the development of a treatment strategy for patients with hepatic hypovascular nodules.
- The hepatic hypovascular nodules that show hyperintensity on T2-weighted images, or that show a higher growth rate should be considered for more frequent follow-up or biopsy.

The aims of our study were to identify patient characteristics and MR imaging findings associated with subsequent hypervascularization in hypovascular nodules that show hypointensity on gadoxetic acid–enhanced hepatobiliary phase MR images in patients with chronic liver diseases.

Materials and Methods

Study Group

Retrospective data collection and analysis were approved by the institutional review board of the two participating hospitals, and the requirement for informed consent was waived. The selection of the subjects is outlined in Figure 1. From February 2008 to October 2010, there were 238 patients who underwent multiple gadoxetic acid–enhanced MR imaging examinations for HCC surveillance. Of these, we excluded patients with *(a)* Child-Pugh class C, owing to insufficient enhancement on gadoxetic acid–enhanced hepatobiliary phase MR images (1), and *(b)* those who had undergone previous systemic chemotherapy or treatment with molecularly targeted agents against malignant tumors. One radiologist (S. Kumano, with 22 years of experience in abdominal imaging) and one gastroenterologist

Published online
10.1148/radiol.12112677 **Content code:** GI

Radiology 2013; 266:480–490

Abbreviations:
CI = confidence interval
HCC = hepatocellular carcinoma
HR = hazard ratio
TVDT = tumor volume doubling time

Author contributions:
Guarantors of integrity of entire study, T.H., T. Murakami; study concepts/study design or data acquisition or data analysis/interpretation, all authors; manuscript drafting or manuscript revision for important intellectual content, all authors; approval of final version of submitted manuscript, all authors; literature research, T.H., Y.I., M.O., Y.K., S. Kumano, M.K., T. Murakami; clinical studies, T.H., Y.I., M.O., Y.K., S. Kogita, M.K.; statistical analysis, T.H., Y.I., M.H.; and manuscript editing, T.H., T. Murakami, Y.I., M.O., M.H., T. Mochizuki.

Conflicts of interest are listed at the end of this article.

Figure 1

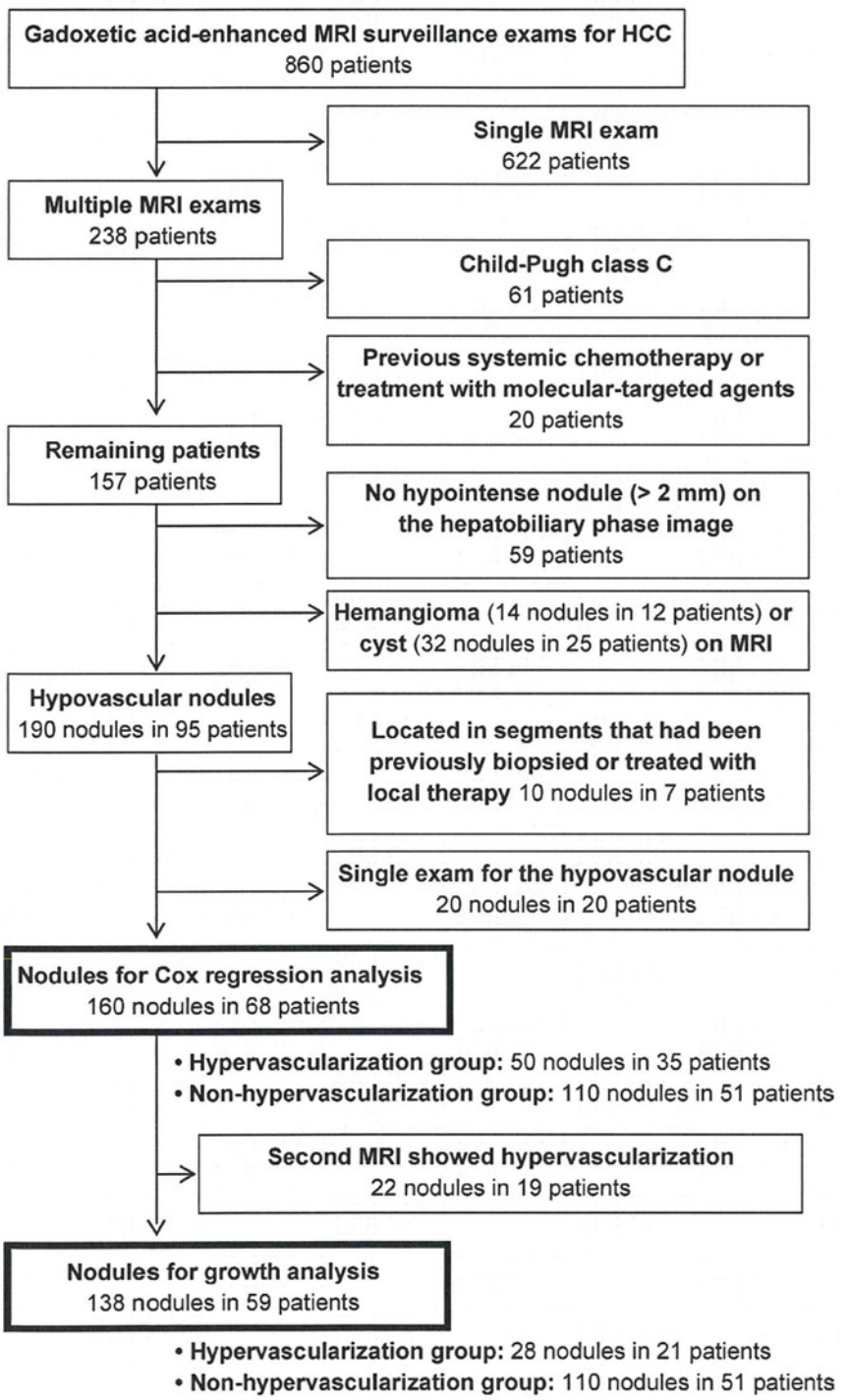

Figure 1: Flowchart of the study population.

specializing in hepatology (Y.I., with 30 years of experience) reviewed images to detect hypovascular nodules and to diagnose subsequent hypervascularization in consensus. A hypovascular nodule was defined as that in which all parts of the nodule showed lower signal intensity than the surrounding liver parenchyma during the arterial phase of dynamic imaging when any of the available modalities were used (intravenous contrast-enhanced CT, CT hepatic arteriography and contrast-enhanced ultrasound) compared with the corresponding site on the unenhanced image. The arterial enhancement was assessed by means of visual inspection. In addition, the subjects were limited to those with round hypointense lesions on gadoxetic acid–enhanced hepatobiliary phase MR images. Procedures involving all modalities were performed within 2 weeks of each other. Nodules were excluded if they were *(a)* less than 2 mm in diameter; *(b)* considered to be suspicious for hemangiomas, cysts or cystic tumors on the basis of other MR imaging sequences or modalities; or *(c)* located in segments that had been previously biopsied or treated with local therapy (including transcatheter arterial chemoembolization).

We identified 160 hypovascular nodules in 68 patients (mean patient age ± standard deviation, 70.0 ± 7.8 years; range, 51–85 years). Among these patients, 48 were men (mean age, 69.9 ± 7.7 years; range, 54–85 years), and 20 were women (mean age, 70.2 ± 8.4 years; range, 51–79 years). The presumed causes of chronic liver disease of the patients were chronic hepatitis C viral infection (n = 46), chronic hepatitis B viral infection (n = 12), alcohol abuse (n = 4), nonalcoholic steatohepatitis (n = 1) and unknown cause (n = 5). Forty (27%) patients had cirrhosis. The number of nodules per patient ranged from one to 10, with a mean value of 2.3. The date of entry into the study was defined as the date of the initial gadoxetic acid–enhanced MR imaging examination. All patients were treated according to the clinical guidelines for the diagnosis and treatment of HCC in Japan (15). During the study period, all patients

received follow-up gadoxetic acid–enhanced MR imaging examinations in combination with US, CT, or angiography at various times according to the degree of liver disease. One radiologist (S. Kumano) and one gastroenterologist who specializes in hepatology (Y.I.) reviewed images in consensus to verify lesion correspondence between the different imaging modalities. Each nodule was followed up until it showed early enhancement when imaged by means of any of the imaging modalities, until the segment containing the nodule was biopsied or treated, or until the final imaging examination of the study period. The number of gadoxetic acid–enhanced MR imaging examinations reviewed per patient was two for 32 patients (43%), three for 16 patients (28%), four for 12 patients (18%), five for three patients (4%), six for three patients (4%), seven for one patient (1%) and eight for one patient (1%). The mean interval between gadoxetic acid–enhanced MR imaging examinations was 186 days ± 110 (range, 57–619 days). Of the 110 nodules that did not develop into hypervascular nodules, 101 were censored at the date of the most recent consultation before November 1, 2010, and nine (in five patients) were censored at the date of the final imaging examination of the study period before therapy (six nodules for transarterial chemoembolization; one each for radiofrequency ablation, intra-arterial reservoir chemotherapy and whole-liver radiation therapy due to coexistent HCC) of the liver segment(s) involved.

We obtained the baseline clinical data by means of review of all available medical records for assessment of the association with the subsequent hypervascularization. The clinical data comprised seven patient characteristics at the time of baseline MR imaging and six initial gadoxetic acid–enhanced MR imaging findings from each nodule (see the Imaging Analysis subsection). Patient characteristics that were used in the study were age, sex, Child-Pugh classification, cause of liver disease, serum α-fetoprotein level, history of local therapy for HCC, and coexistence of hypervascular HCC. For patients with hepatitis B infections, we recorded information regarding the use of oral nucleotide analogs with activity against hepatitis B. The mean interval between the laboratory test and initial MR imaging examination was 9 days (range, 0–24 days).

Nodules were categorized into two groups according to the presence (hypervascularization group) or absence (nonhypervascularization group) of early enhancement at the final imaging examination. Needle biopsy specimens were reviewed by two expert pathologists who made a consensus diagnosis according to the International Working Party criteria (9).

Imaging Techniques

MR imaging studies were performed by using either a 3.0 T (Achieva; Philips Medical Systems, Best, Netherlands) or one of two 1.5 T systems (Signa Excite HDxt; GE Healthcare, Milwaukee, Wis; Gyroscan Intera Nova; Philips Medical Systems) (Table 1). First, a T1-weighted dual-echo sequence was performed. For dynamic imaging, T1-weighted three-dimensional fat-suppressed gradient-echo images were acquired before and after a bolus injection of 0.025 mmol/kg of body weight of gadoxetic acid (EOB-Primovist; Bayer Schering Pharma, Osaka, Japan) at a rate of 2 mL/sec with a saline flush through the antecubital vein. Arterial-phase imaging was performed by using a bolus tracking technique: the center of k-space was acquired 15 seconds after the contrast material appeared in the abdominal aorta (16). Portal venous and hepatobiliary phase images were acquired after an imaging delay of 70 seconds and 20 minutes, respectively. T2-weighted images were acquired with a fat-suppressed fast spin-echo sequence before or within 10 min after contrast-material injection. Although there were missing data from the fat-suppressed T2-weighted fast spin-echo images (not available owing to motion artifacts in two nodules; other T2-weighted sequences were obtained for 32 nodules), we included all subjects in the analysis. Dynamic contrast-enhanced CT, CT hepatic arteriography and contrast-enhanced US were performed as described in the literature (17–19).

Image Analysis

A consensus review of baseline MR images was performed by three radiologists (M.O., T.H., and Y.K., with 18, 11, and 6 years of experience in abdominal imaging, respectively), who were blinded to the outcomes and the biopsy results for each nodule. The fat content of each nodule was determined on the basis of T1-weighted dual-echo images according to apparent signal loss on opposed-phase images relative to in-phase images. On the T2-weighted images, each lesion was evaluated for signal intensity relative to that of the surrounding liver parenchyma and classified as hyperintense, isointense, hypointense or missing. On the T1-weighted three-dimensional fat-suppressed gradient-echo images of without and with contrast enhancement (hepatobiliary phase), signal intensities of the nodule and liver parenchyma were recorded to evaluate nodule-to-liver contrast ratios. For measurement of the nodule, one abdominal radiologist (T.H.) placed the largest possible region of interest but did not include the edges of the nodule to avoid edge artifacts. For the liver parenchyma, two regions of interest that avoided the major hepatic and portal vessels (size range, 200–400 mm^2) were selected, and then the mean value was calculated. The nodule-to-liver contrast ratios were calculated for each unenhanced and hepatobiliary phase image by dividing the signal intensity of the nodule by the signal intensity of the liver parenchyma. The contrast enhancement ratio was then calculated by dividing the contrast ratios of the hepatobiliary phase images by those of the unenhanced images.

One abdominal radiologist (T.H.) measured the maximum nodule diameter on axial gradient-echo T1-weighted gadoxetic acid–enhanced hepatobiliary-phase images of the baseline and the final MR imaging examinations. Only for the purpose of the growth analysis, the final MR imaging examination was defined as the last MR imaging examination before hypervascularization for each nodule. Twenty-two nodules in which the second MR imaging examination showed hypervascularization (19 pairs of examinations; median interval between the two examinations, 210 days;

Table 1

Pulse Sequence Parameters for 1.5-T and 3.0-T Imaging

	T1-weighted Dual-Echo GRE*		Fat-suppressed 3D T1-weighted GRE		Fat-suppressed T2-weighted Fast Spin-Echo	
Parameter	1.5 T 2D†	3.0 T 3D‡	1.5 T†	3.0 T‡	1.5 T†	3.0 T‡
Breathing	Breath hold	Breath hold	Breath hold	Breath hold	Respiratory-triggered technique	Respiratory-triggered technique
Matrix	256 × 256, 320 × 192	192, 176	320 × 512, 320 × 192	320 × 256, 320 × 192	512 × 272, 256 × 224	400, 400
Section thickness (mm)	8, 3.5	7, 7	5, 5	2.5, 3	8, 7	6, 6
Intersection gap (mm)	0.8, 0	0, 0	−2.5, −2.5	−1.25, −1.5	0.8, 1.4	1, 1
Repetition time (msec)	200, 200	3.9, 3.8	4.4, 4.3	3.5, 3.5	>2000, >2000	>3000, >3000
Echo time (msec) in/opposed	4.6/2.3, 4.3/2.1	1.17/2.5, 1.17/2.5	2.2, 2.1	1.7, 1.7	80, 105	80, 80
Flip angle/refocusing angle (degrees)	70, 70	10, 10	10, 12	10, 10	180, 180	160, 160
Reduction factor	1.8, 2	2, 2	1.8, 2	2, 1.9	0, 2	1.6, 2

Note.—Field of view was 250–270 mm × 350–380 mm (adjusted for each patient). 2D = two dimensional, 3D = three dimensional, GRE = gradient-recalled echo.

* Indicates in- and opposed-phase imaging.

† For the 1.5-T system, a 16-channel and an 8-channel phased-array body coil were used. Data are presented as 16 channel/8 channel.

‡ For the 3-T system, a 6-channel body coil and 32-channel cardiac coil were used and adjusted to the patient's physique. Data are presented as 6 channel/32 channel.

range, 91–410 days) were excluded from the growth analysis, because the growth rate before hypervascularization could not be calculated. Thus, 138 nodules from 59 patients were included in the growth analysis. First, the tumor volume doubling time (TVDT) was calculated as follows (20,21): $TVDT = T \times \log 2/[3 \times \log(D_2/D_1)]$, where T is the time interval between two measurements and D_1 and D_2 denote the maximum diameter of the nodule at the initial and last MR imaging examinations, respectively. Then, the growth rate of the nodules was calculated as the inverse of the TVDT.

Statistical Analysis

All analyses were conducted at the nodule level. R software (Version 2.12.0; R Foundation for Statistical Computing, Vienna, Austria) was used for statistical analysis (22). To evaluate the independent prognostic significance of baseline covariates for subsequent hypervascularization, a multivariate Cox proportional hazard model was used. Because 32 patients had multiple nodules detected at two or more follow-up examinations, we used the coxph function from the survival package in the R software, with the cluster option. This method allows accounting for correlation induced by having multiple nodules per patient and uses robust variance estimates (23). Before model selection, bivariate analysis was performed by using Spearman rank correlations to test for collinearity among independent variables. As a result, Spearman correlation coefficients for variables were generally below 0.5, which suggests that multicollinearity was not of concern. Hazard ratios (HRs) and 95% confidence intervals (CIs) were calculated. Because no factor (except intensity on T2-weighted images) was found to show a significant difference when univariate analysis was performed, preliminary multivariate Cox proportional hazards models were constructed by using all 13 variables. Candidate variables were then allowed to enter the final model (entry criterion, $P < .05$). Fat content and initial diameter were forced into the final model because they were considered important predictors (12). The Wald test was performed to determine an overall P value for each variable, and a robust score test was used to assess the significance of the final model as a whole. The model that was fitted by using missing data was not appreciably different from that with the missing data excluded.

The median time interval between the initial and final MR imaging examination was compared for the two groups by using the Mann-Whitney U test. For evaluation of initial diameter and growth rate of the nodules, continuous data differences between the two groups were tested with the Mann-Whitney U test, and categorical data were assessed by using the χ^2 test. Correlation between the initial diameter and the growth rate of the nodules was examined by using the Kendall tau rank test. The prognostic value of the growth rate was evaluated by means of the area under the receiver operating characteristic curve. By using the ROCR package in the R software, the cutoff value for the growth rate was determined at the optimal operating point, with the highest sensitivity and specificity combined (24). Cumulative event rates were estimated by using the Kaplan-Meier method and compared by using the log rank statistic. A P value of less than .05 was considered to indicate a statistically significant difference. All P values were two-sided.

Results

Study Population and Events

During the median follow-up time of 342 days (range, 64–948 days), arterial hypervascularization was observed in 31% (50 of 160) of the nodules in 52% (35 of 68) of the patients. The cumulative percentages of nodules that showed

Table 2

Baseline Patient Characteristics and MR Imaging Findings of 160 Nodules

Parameter	No. of Nodules	Hypervascularization at Follow-up		Preliminary Multivariate Cox Model	
		Yes ($n = 50$)	No ($n = 110$)	HR (95% CI)	*P* Value
Patient characteristic					
Age (y)	...	70.5 ± 7.6 (58–85)*	70.4 ± 8.3 (51–84)*	1.0 (0.9, 1.1)	.852
Sex	...				.326
Men	106	32 (30)	74 (70)	1.0	
Women	54	18 (33)	36 (67)	1.4 (0.7, 3.1)	
Child-Pugh class					.005
A or chronic hepatitis	146	44 (30)	102 (70)	1.0	
B	14	6 (43)	8 (57)	3.8 (1.5, 9.0)	
Etiology of liver disease					.019
Hepatitis C virus	107	35 (33)	72 (67)	1.0 (0.3, 3.1)	
Hepatitis B virus	26	6 (23)	20 (77)	0.2 (0.03, 0.8)	
Non-B, non-C (ref)	27	9 (33)	18 (67)	1.0	
Serum α-fetoprotein level > 20 ng/mL	66	24 (36)	42 (64)	0.9 (0.5, 2.0)	.948
History of local therapy for HCC	129	46 (36)	83 (64)	5.5 (2.1, 14.7)	<.001
Coexistence of hypervascular HCC	67	29 (43)	38 (57)	2.0 (1.1, 3.7)	.022
MR Imaging Finding					
Fat-suppressed T2-weighted fast spin echo†					<.001
Hyperintensity	18	10 (56)	8 (44)	9.4 (3.6, 24.5)	
Iso- or hypointensity (ref)	108	25 (23)	83 (77)	1.0	
Missing data	34	15 (34)	19 (56)	3.7 (1.7, 8.0)	
Fat containing on in- and opposed-phase images†	24	10 (42)	14 (58)	1.4 (0.6, 3.4)	.491
Noise-to-liver contrast on unenhanced fat-suppressed T1-weighted GRE images	...	0.95 ± 0.14 (0.66–1.3)*	0.97 ± 0.17 (0.49–1.9)*	0.05 (0.1×10^{-4}, 1.7×10^{2})	.464
Noise-to-liver contrast on hepatobiliary phase fat-suppressed T1-weighted GRE images	...	0.69 ± 0.13 (0.31–0.99)*	0.71 ± 0.11 (0.46–0.95)*	47.5 (6.8×10^{-4}, 3.3×10^{6})	.489
Gadoxetic acid contrast-enhancement ratio	...	0.74 ± 0.14 (0.40–0.98)*	0.75 ± 0.14 (0.42–1.5)*	0.07 (0.1×10^{-5}, 3.8×10^{5})	.629
Diameter (mm)	...	9.5 ± 5.1 (2–34)*	9.8 ± 3.7 (4–21)*	1.0 (0.9, 1.1)	.998

Note.—Unless otherwise indicated, data are numbers of patients, with percentages in parentheses. GRE = gradient-recalled echo, ref = referent category.

* Data are mean ± standard deviation, with range in parentheses.

† Qualitative assessment.

hypervascularization at 6, 12, 18, and 24 months were 10%, 25%, 36%, and 46%, respectively. Hypervascularization was diagnosed in 39 nodules on the basis of arterial-phase gadoxetic acid–enhanced MR images, eight nodules on the basis of dynamic CT images, two nodules on the basis of CT hepatic arteriographic images, and one nodule on the basis of contrast-enhanced US. In the hypervascularization group, the mean number of hypervascularized nodules was 1.5 (range, 1–7) per patient during the study period.

Histologic results from core needle biopsy were obtained for 13 nodules. Of these, nine nodules were in the hypervascularization group (eight well-differentiated HCCs and one moderately differentiated HCC). Three nodules in the nonhypervascularization group were diagnosed as dysplastic nodules and one as well-differentiated HCC.

Baseline Findings

Table 2 shows the baseline characteristics of the 160 nodules and results of the preliminary multivariate Cox regression. In the final model, five of the variables showed a statistically significant difference (robust score test, $P = .023$; Table 3). The factors associated with an increased risk of hypervascularization were hyperintensity on T2-weighted images (HR = 8.7; 95% CI: 3.6, 20.8), previous local therapy for HCC (HR = 5.0; 95% CI: 1.8, 13.6), Child-Pugh class B cirrhosis (HR = 3.6; 95% CI: 1.4, 9.5), and coexistence of hypervascular HCC (HR = 2.0; 95% CI: 1.0, 3.8). Hepatitis B infection was independently associated with a decreased risk (HR = 0.2; 95% CI: 0.04, 0.8). Of 26 nodules in 13 patients with chronic hepatitis B infections, 23 nodules in 11 patients were treated with oral nucleotide analogs with activity against hepatitis B at the point of entry (five of six nodules in the hypervascularization group and 18 of 20 nodules in the nonhypervascularization group). Fat content and the initial diameter of the nodule were not substantially different in the final model. Of 14 fat-containing nodules in the nonhypervascularization

group, four nodules in one patient were censored because the patient underwent transcatheter arterial chemoembolization for HCC in a different liver segment. Two nodules were censored because of biopsy; one was diagnosed as moderately differentiated HCC, and the other was a dysplastic nodule. The mean initial nodule diameter was not significantly different between the hypervascularization (9.5 mm ± 5.1 [range, 2–34 mm]) and the nonhypervascularization groups (9.8 mm ± 3.7 [range, 4–21 mm]) (P = .282). The numbers of nodules that were smaller than 5 mm, 5–10 mm, 10–15 mm, and greater than 15 mm in initial size were four, 28, 11, and seven in the hypervascularization group, and three, 60, 33, and 14 in the nonhypervascularization group, respectively. In addition, there was no difference in the percentage of nodules greater than or equal to 15 mm in size between the two groups (14% [seven of 50] vs 13% [14 of 110], respectively; P = .825).

Table 3

Multivariate Predictors of Subsequent Hypervascularization

Variable	HR (95% CI)	*P* Value
Significant independent predictors		
Child-Pugh classification		.008
A or chronic hepatitis	1.0	
B	3.6 (1.4, 9.5)	
Cause of liver disease		.017
Hepatitis C virus	1.1 (0.4, 3.1)	
Hepatitis B virus	0.2 (0.04, 0.8)	
Non-B and non-C liver disease (Ref)	1.0	
History of local therapy for HCC	5.0 (1.8, 13.6)	.002
Coexistence of hypervascular HCC	2.0 (1.0, 3.8)	.038
Fat-suppressed T2-weighted fast spin echo		<.001
Hyperintensity	8.7 (3.6, 20.8)	
Hypo- or isointensity (Ref)	1.0	
Missing data	3.4 (1.4, 7.9)	
Additional variables included in the model		
Fat containing on in- and opposed-phase images	1.3 (0.5, 3.7)	.567
Diameter (mm)	1.0 (0.9, 1.1)	.692

Growth Analysis

Twenty-eight lesions in the hypervascularization group (initial diameter, 9.7 mm ± 5.9 [range, 2–34 mm]) and 110 nodules (9.8 mm ± 3.7 [range, 4–21 mm]) in the nonhypervascularization group were evaluated. The median time between the initial and last MR imaging examination was not significantly different (P = .075) between the two groups (235 and 293 days, respectively). In the hypervascularization group, 27 nodules increased in diameter during follow-up (Fig 2) and one remained stable. The mean growth rate in the hypervascularization group (6.5×10^{-3}/day [TVDT, 154 days]) was significantly higher ($P = 1.8 \times 10^{-6}$) than that in the nonhypervascularization group (1.1×10^{-3}/day [TVDT, 946 days]) (Fig 3). There was no correlation between initial diameter and growth rate (Kendall tau = −0.066; P = .266) (Fig 4). Receiver operating characteristic analysis (area under the curve, 0.79) identified a growth rate cutoff value of 1.8×10^{-3} per day (TVDT, 542 days) with a positive predictive value of 89% (25 of 28 nodules) and a negative predictive value of 63% (70 of 110 nodules) for hypervascularization (Fig 5, *A*). The 1-year cumulative proportion of nodules showing hypervascularization was 0% for those with a growth rate of less than 1.8×10^{-3}/day and 53% for those with a growth rate greater than or equal to 1.8×10^{-3}/day (log-rank test, $P = 5.2 \times 10^{-8}$; Fig 5, *B*).

Discussion

We set out to determine risk factors associated with hypervascularization in hypovascular nodules in patients with chronic liver diseases by using time-to-event analysis. Among the baseline patient characteristics and MR imaging findings, the most important variable associated with an increased risk of hypervascularization was hyperintensity on T2-weighted images. In the hypervascularization group, higher signal intensity on T2-weighted images might reflect peliotic changes in the intratumoral sinusoids of HCC (25). Meanwhile, nodular regeneration, fibrosis, and scarring that occur in the course of cirrhosis occasionally appear as hyperintense round lesions on T2-weighted images. Dysplastic nodules can be hyperintense on T2-weighted images; the causes are considered to be varying degrees of fibrosis, or infarction (26,27). It has been reported that T2-weighted imaging does not provide added diagnostic value to gadoxetic acid–enhanced images for the detection and characterization of focal lesions in cirrhotic livers (28). Findings from our study suggest that the combination of T2-weighted images and gadoxetic acid–enhanced MR images could be useful in the prediction of hypervascularization of previously hypovascular nodules.

Child-Pugh class B cirrhosis increased the risk of hypervascularization compared with Child-Pugh class A or chronic hepatitis, and hepatitis B infection decreased the risk compared with hepatitis C infection. These results might reflect the epidemiologic features of HCC (29,30); Child-Pugh class B and C are associated with a three-fold increase in the risk of HCC. The annual incidence of HCC in patients with cirrhosis due to hepatitis B infection exceeds 2%, which is lower than that due to hepatitis C infection (3%–8%). In addition, there may be morphologic and histologic differences between hypovascular nodules associated with hepatitis B and those associated with hepatitis C infection.

Figure 2

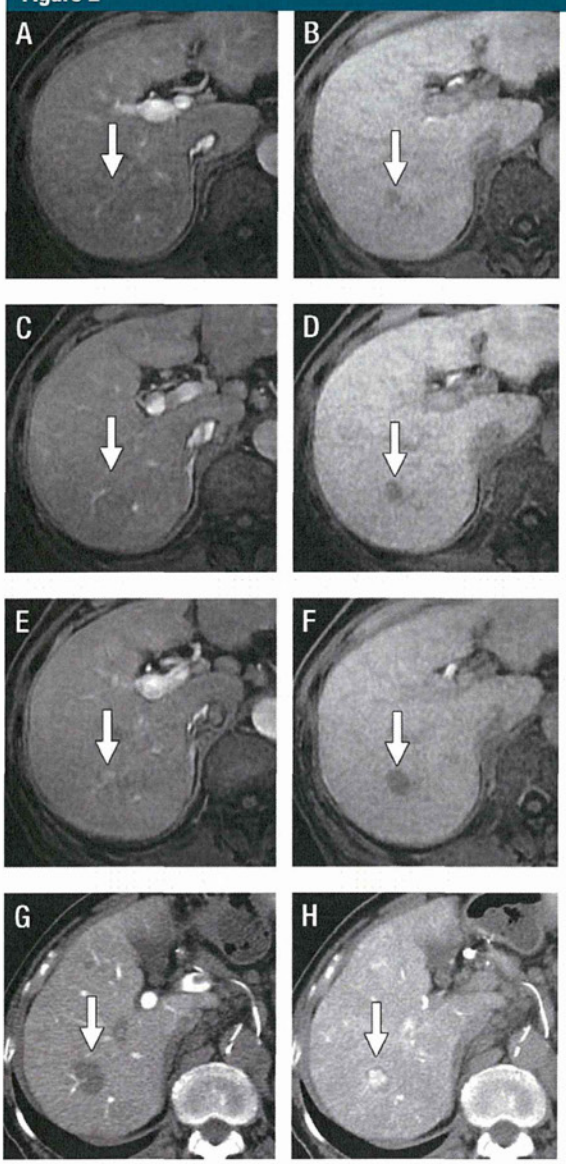

Figure 2: Growing hypovascular hepatic nodule (arrows) and subsequent hypervascularization in an 86-year-old man with hepatitis C and Child-Pugh class B cirrhosis. *A-F*, Axial gadoxetic acid–enhanced T1-weighted fat-suppressed three-dimensional gradient-recalled echo images obtained during (*A*, *C*, and *E*) arterial phase and (*B*, *D*, *F*) hepatobiliary phase obtained at (*A*, *B*) baseline, (*C*, *D*) day 94, and (*E*, *F*) day 176. At (*A*) baseline and (*C*) day 94, hepatic nodule in right posterior section showed neither arterial-phase enhancement nor portal-venous phase washout. Hepatobiliary phase images showed that maximum diameter increased from 8 mm at, *B*, baseline to 12 mm at, *D*, day 94, and TVDT was calculated as 170 days. *E*, Arterial-phase image at day 176 shows partial enhanceme of nodule. *G*, At day 194, CT arterial portographic image shows a well-defined, round perfusion defect and, *H*, CT hepatic arteriographic image shows marked enhancement corresponding to nodule. Nodule was diagnosed as HCC on the basis of image views and tumor markers.

Figure 3

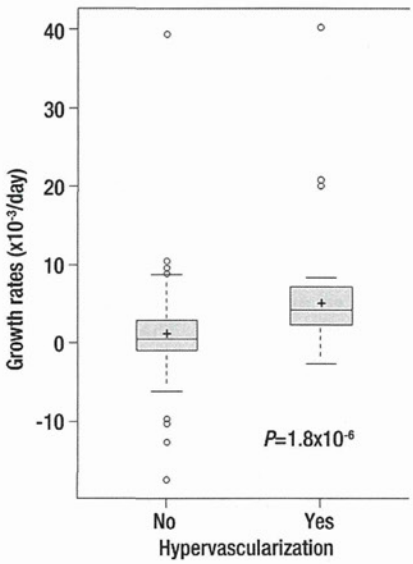

Figure 3: Box plot shows distribution of growth rates of 138 nodules. Median values and 25th and 75th percentiles are shown in each box plot. Vertical bars represent largest and smallest values that are not outliers. + = Mean; ○ = outlier of more than 1.5 times box length.

In comparison with hepatitis C infection or alcohol abuse, hepatitis B infection tends to induce macronodular (> 3 mm) cirrhosis (31). Thus, macronodular benign nodules in cases of hepatitis B cirrhosis might have been present in our subjects. Another possible reason why hepatitis B infection was a negative predictor for hypervascularization might be that antihepatitis B nucleoside analogs prevented the development of HCC (32).

The nodule-to-liver contrast ratios on unenhanced T1-weighted images and gadoxetic acid–enhanced hepatobiliary phase MR images were not a significant prognostic factor, which is consistent with previous reports (33). The signal intensity of nodules on T1-weighted images may be affected by intratumoral fat, metal, or glycogen in the surrounding hepatic parenchyma (1,34). The fat content of the nodules was also not a significant predictor of hypervascularization in our study. One possible reason for this was the fact that both early HCCs and dysplastic nodules could appear as intracellular lipid-containing lesions in cirrhotic livers (35). There was also no statistically significant association between initial diameter and hypervascularization in our study results. The probable reason for this was that most subjects (87%) had nodules of less than 15 mm in diameter (139 of 160 nodules).

The reported TVDT for HCC ranges from 18 to 605 days (1). The mean growth rate for HCCs smaller than 20 mm that showed no hyperintensity on T2-weighted MR images but that enhanced during arterial phase MR imaging was 10.5×10^{-3}/day (TVDT, 95 days; calculated by using data from Jeong et al [36]). The hypervascularization group, which was considered to be representative of an earlier stage of multistep carcinogenesis, showed the lower mean growth rate (6.5×10^{-3}/day [TVDT, 154

Figure 5

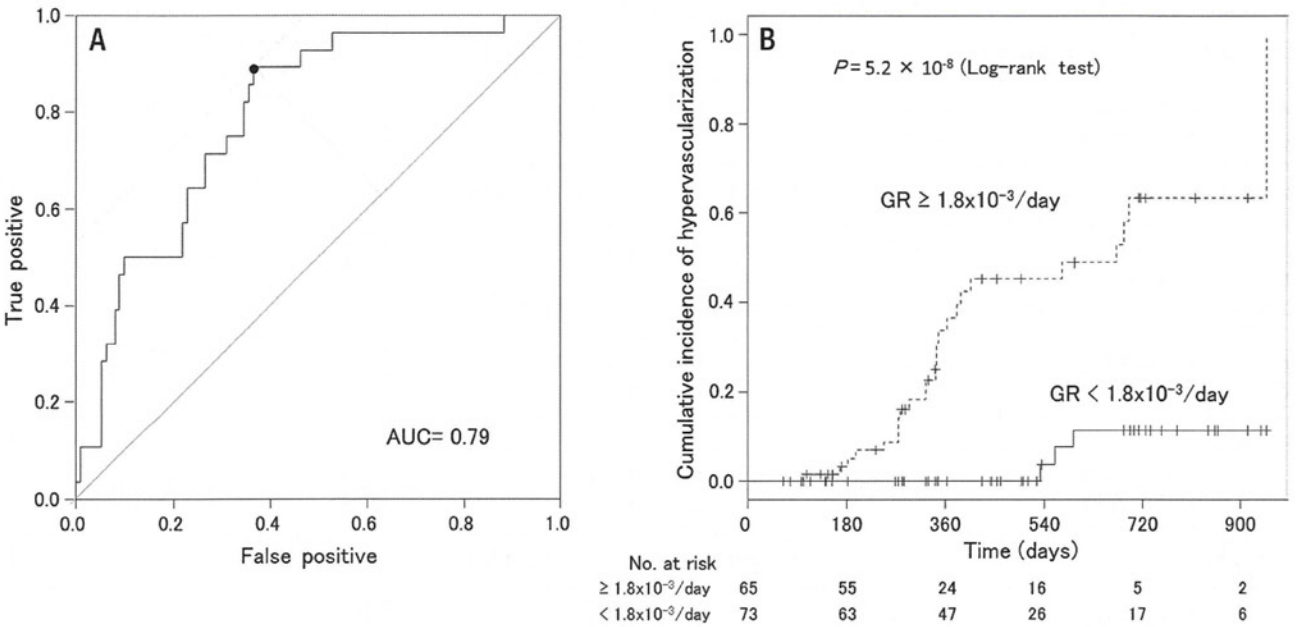

Figure 5: *A*, Graph shows receiver operating characteristic curve of growth rate *(GR)* for the prediction of hypervascularization (area under the curve *[AUC]*, 0.79). The optimal operating point on the receiver operating characteristic curve is marked with a black dot (growth rate, 1.8×10^{-3}/day). *B*, Kaplan-Meier analysis shows effect of growth rate on cumulative incidence of hypervascularization. Number of nodules at risk at each time point is shown at bottom of figure.

days]) than that reported in the Jeong et al study (36).

On the basis of these previous studies, hypovascular nodules larger than 15 mm are considered appropriate for biopsy. In cases with nodules less than 10 mm in diameter, the American Association for the Study of Liver Disease recommends imaging follow-up at 3–6 month intervals, with careful attention to increases in size or changes in vascular pattern. Repeated biopsy for nodules larger than 10 mm can be performed, but a needle liver biopsy has some disadvantages including inaccurate sampling caused by technical difficulties (eg, poor lesion or needle visualization, deeply located lesions, and hepatic fibrosis), risk of bleeding, and needle track seeding. Our growth analysis, along with baseline risk factors, might improve diagnostic discrimination with or without the need for biopsy, particularly for nodules measuring 10–15 mm. By using a cutoff growth rate of 1.8×10^{-3}/day (TVDT, 542 days), the calculated diameters at

Figure 4

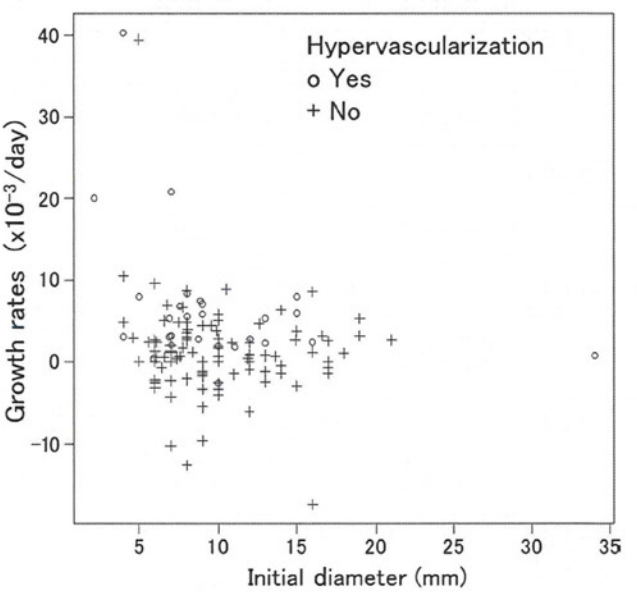

Figure 4: Scatterplot shows growth rate above the initial diameter. Individual nodules were coded according to whether they showed subsequent hypervascularization during the study period.

the 6-month follow-up examination for nodules with an initial diameter of 10, 11, 12, 13, and 14 mm were 10.8, 11.9, 13.0, 14.0, and 15.1 mm, respectively. We suggest that nodules with the risk factors for hypervascularization or those showing faster growth may justify more frequent follow-up or biopsy. If growth is slower, biopsy may not be needed, although the absence of growth does not rule out malignancy. According to expert opinion, nodules are declared benign only if they regress or remain stable for 2 years (37).

The reported incidence rates of hypervascularization vary throughout different studies. In our study, the overall 6- and 12-month cumulative percentages for hypervascularization were 10% and 25%, respectively, which is lower than the percentages calculated by Kumada et al (27.6% and 43.5%, respectively) (13). This may be partially explained by time frame, sample size, and/or follow-up policy of subjects in each study.

Our study had some limitations. It was a retrospective study, and this fact may have introduced bias in data homogeneity. To minimize sampling bias, we collected data from consecutive patients who underwent multiple gadoxetic acid–enhanced MR imaging examinations in two hospitals. Also, the duration of disease and date of diagnosis were potentially important confounders. However, they were not available for retrospective review.

Regarding the imaging technique, a relatively high rate (2 mL/sec) of injection of gadoxetic acid might reduce the performance of arterial-phase imaging. Some reports suggested that a lower injection rate might be appropriate owing to stretching the bolus without reducing the enhancement peak (38,39). However, we performed gadoxetic acid–enhanced MR imaging with optimized imaging technique (40) and timing (16) to acquire good images in the arterial phase.

On imaging analysis, our study was potentially limited by consensus review because we did not assess interobserver variability. Also, in the case of smaller nodules (< 10 mm), it might be difficult to obtain a clear correspondence between the MR images and those of the other modalities (CT, and in particular, contrast-enhanced US), even though well-trained radiologists and physicians reviewed the images.

Tumor growth kinetic calculations were based on the general assumption that tumor cells grow exponentially. This assumption might not hold true owing to fibrosis or to the intracellular lipid content of both the hepatic nodules and surrounding cirrhotic liver parenchyma. Because patients with Child-Pugh class C cirrhosis were excluded, the influence of fibrosis of the surrounding parenchyma is limited. Also, measurement errors associated with manual evaluation may have led to bias. However, to improve accuracy all measurements were performed in the same manner, by using T1-weighted three-dimensional gradient-echo images that provided high spatial resolution (7). A large-scale prospective validation study is necessary to confirm our proposed cutoff values.

In conclusion, hypervascularization occurs in about one-third of the hypovascular nodules that show hypointensity on gadoxetic acid–enhanced hepatobiliary phase MR images. MR imaging findings, including hyperintensity on T2-weighted images and a higher growth rate, may predict arterial hypervascularization, which may lead to early diagnosis and treatment of HCC.

Disclosures of Conflicts of Interest: T.H. Financial activities related to the present article: Received Osaka Cancer Foundation grant in 2010. Financial activities not related to the present article: none to disclose. Other relationships: none to disclose. **T. Murakami** No relevant conflicts of interest to disclose. **Y.I.** No relevant conflicts of interest to disclose. **M.O.** No relevant conflicts of interest to disclose. **M.H.** No relevant conflicts of interest to disclose. **Y.K.** No relevant conflicts of interest to disclose. **S. Kogita** No relevant conflicts of interest to disclose. **S. Kumano** No relevant conflicts of interest to disclose. **M.K.** No relevant conflicts of interest to disclose. **T. Mochizuki** No relevant conflicts of interest to disclose.

References

1. Willatt JM, Hussain HK, Adusumilli S, Marrero JA. MR Imaging of hepatocellular carcinoma in the cirrhotic liver: challenges and controversies. Radiology 2008;247(2):311–330.
2. Bruix J, Sherman M; American Association for the Study of Liver Diseases. Management of hepatocellular carcinoma: an update. Hepatology 2011;53(3):1020–1022.
3. Giovagnoni A, Paci E. Liver. III: Gadolinium-based hepatobiliary contrast agents (Gd-EOB-DTPA and Gd-BOPTA/Dimeg). Magn Reson Imaging Clin N Am 1996;4(1):61–72.
4. Bluemke DA, Sahani D, Amendola M, et al. Efficacy and safety of MR imaging with liver-specific contrast agent: U.S. multicenter phase III study. Radiology 2005;237(1):89–98.
5. Haradome H, Grazioli L, Tinti R, et al. Additional value of gadoxetic acid-DTPA-enhanced hepatobiliary phase MR imaging in the diagnosis of early-stage hepatocellular carcinoma: comparison with dynamic triple-phase multidetector CT imaging. J Magn Reson Imaging 2011;34(1):69–78.
6. Okada M, Imai Y, Kim T, et al. Comparison of enhancement patterns of histologically confirmed hepatocellular carcinoma between gadoxetate- and ferucarbotran-enhanced magnetic resonance imaging. J Magn Reson Imaging 2010;32(4):903–913.
7. Lee VS, Lavelle MT, Rofsky NM, et al. Hepatic MR imaging with a dynamic contrast-enhanced isotropic volumetric interpolated breath-hold examination: feasibility, reproducibility, and technical quality. Radiology 2000;215(2):365–372.
8. Golfieri R, Renzulli M, Lucidi V, Corcioni B, Trevisani F, Bolondi L. Contribution of the hepatobiliary phase of Gd-EOB-DTPA-enhanced MRI to Dynamic MRI in the detection of hypovascular small (≤ 2 cm) HCC in cirrhosis. Eur Radiol 2011;21(6):1233–1242.
9. International Consensus Group for Hepatocellular NeoplasiaThe International Consensus Group for Hepatocellular Neoplasia. Pathologic diagnosis of early hepatocellular carcinoma: a report of the international consensus group for hepatocellular neoplasia. Hepatology 2009;49(2):658–664.
10. Hayashi M, Matsui O, Ueda K, et al. Correlation between the blood supply and grade of malignancy of hepatocellular nodules associated with liver cirrhosis: evaluation by CT during intraarterial injection of contrast medium. AJR Am J Roentgenol 1999;172(4):969–976.
11. Yu JS, Chung JJ, Kim JH, Kim KW. Fat-containing nodules in the cirrhotic liver: chemical shift MRI features and clinical implications. AJR Am J Roentgenol 2007;188(4):1009–1016.
12. Motosugi U, Ichikawa T, Sano K, et al. Outcome of hypovascular hepatic nodules revealing no gadoxetic acid uptake in patients

with chronic liver disease. J Magn Reson Imaging 2011;34(1):88–94.

13. Kumada T, Toyoda H, Tada T, et al. Evolution of hypointense hepatocellular nodules observed only in the hepatobiliary phase of gadoxetate disodium-enhanced MRI. AJR Am J Roentgenol 2011;197(1):58–63.
14. Sakamoto M, Hirohashi S, Shimosato Y. Early stages of multistep hepatocarcinogenesis: adenomatous hyperplasia and early hepatocellular carcinoma. Hum Pathol 1991;22(2):172–178.
15. Makuuchi M, Kokudo N, Arii S, et al. Development of evidence-based clinical guidelines for the diagnosis and treatment of hepatocellular carcinoma in Japan. Hepatol Res 2008;38(1):37–51.
16. Kagawa Y, Okada M, Kumano S, et al. Optimal scanning protocol of arterial dominant phase for hypervascular hepatocellular carcinoma with gadolinium-ethoxybenzyl-diethylenetriamine pentaacetic acid-enhanced MR. J Magn Reson Imaging 2011;33(4):864–872.
17. Goshima S, Kanematsu M, Kondo H, et al. MDCT of the liver and hypervascular hepatocellular carcinomas: optimizing scan delays for bolus-tracking techniques of hepatic arterial and portal venous phases. AJR Am J Roentgenol 2006;187(1):W25–W32.
18. Hori M, Murakami T, Kim T, Nakamura H. Diagnosis of hepatic neoplasms using CT arterial portography and CT hepatic arteriography. Tech Vasc Interv Radiol 2002; 5(3):164–169.
19. Kudo M, Hatanaka K, Maekawa K. Newly developed novel ultrasound technique, defect reperfusion ultrasound imaging, using sonazoid in the management of hepatocellular carcinoma. Oncology 2010;78(Suppl 1):40–45.
20. Collins VP, Loeffler RK, Tivey H. Observations on growth rates of human tumors. Am J Roentgenol Radium Ther Nucl Med 1956;76(5):988–1000.
21. Schwartz M. A biomathematical approach to clinical tumor growth. Cancer 1961; 14:1272–1294.
22. R Development Core Team. R: A language and environment for statistical computing. Vienna, Austria: R Foundation for Statistical Computing, 2010.
23. Lin DY. Cox regression analysis of multivariate failure time data: the marginal approach. Stat Med 1994;13(21):2233–2247.
24. Fawcett T. An introduction to ROC analysis. Pattern Recognit Lett 2006;27(8):861–874.
25. Kadoya M, Matsui O, Takashima T, Nonomura A. Hepatocellular carcinoma: correlation of MR imaging and histopathologic findings. Radiology 1992;183(3):819–825.
26. Ohtomo K, Baron RL, Dodd GD 3rd, Federle MP, Ohtomo Y, Confer SR. Confluent hepatic fibrosis in advanced cirrhosis: evaluation with MR imaging. Radiology 1993;189(3):871–874.
27. Kim T, Baron RL, Nalesnik MA. Infarcted regenerative nodules in cirrhosis: CT and MR imaging findings with pathologic correlation. AJR Am J Roentgenol 2000;175(4): 1121–1125.
28. Hussain HK, Syed I, Nghiem HV, et al. T2-weighted MR imaging in the assessment of cirrhotic liver. Radiology 2004;230(3): 637–644.
29. Fattovich G, Stroffolini T, Zagni I, Donato F. Hepatocellular carcinoma in cirrhosis: incidence and risk factors. Gastroenterology 2004;127(5,Suppl 1):S35–S50.
30. Bolondi L, Sofia S, Siringo S, et al. Surveillance programme of cirrhotic patients for early diagnosis and treatment of hepatocellular carcinoma: a cost effectiveness analysis. Gut 2001;48(2):251–259.
31. Rozario R, Ramakrishna B. Histopathological study of chronic hepatitis B and C: a comparison of two scoring systems. J Hepatol 2003;38(2):223–229.
32. Matsumoto A, Tanaka E, Rokuhara A, et al. Efficacy of lamivudine for preventing hepatocellular carcinoma in chronic hepatitis B: A multicenter retrospective study of 2795 patients. Hepatol Res 2005;32(3): 173–184.
33. Kobayashi S, Matsui O, Gabata T, et al. Gadolinium ethoxybenzyl diethylenetriamine pentaacetic Acid-enhanced magnetic resonance imaging findings of borderline lesions at high risk for progression to hypervascular classic hepatocellular carcinoma. J Comput Assist Tomogr 2011;35(2): 181–186.
34. Ebara M, Fukuda H, Kojima Y, et al. Small hepatocellular carcinoma: relationship of signal intensity to histopathologic findings and metal content of the tumor and surrounding hepatic parenchyma. Radiology 1999; 210(1):81–88.
35. Basaran C, Karcaaltincaba M, Akata D, et al. Fat-containing lesions of the liver: cross-sectional imaging findings with emphasis on MRI. AJR Am J Roentgenol 2005; 184(4):1103–1110.
36. Jeong YY, Mitchell DG, Kamishima T. Small (<20 mm) enhancing hepatic nodules seen on arterial phase MR imaging of the cirrhotic liver: clinical implications. AJR Am J Roentgenol 2002;178(6):1327–1334.
37. Bruix J, Sherman M; Practice Guidelines Committee, American Association for the Study of Liver Diseases. Management of hepatocellular carcinoma. Hepatology 2005;42(5):1208–1236.
38. Zech CJ, Vos B, Nordell A, et al. Vascular enhancement in early dynamic liver MR imaging in an animal model: comparison of two injection regimen and two different doses Gd-EOB-DTPA (gadoxetic acid) with standard Gd-DTPA. Invest Radiol 2009;44(6):305–310.
39. Chung SH, Kim MJ, Choi JY, Hong HS. Comparison of two different injection rates of gadoxetic acid for arterial phase MRI of the liver. J Magn Reson Imaging 2010;31(2):365–372.
40. Kim KA, Herigault G, Kim MJ, Chung YE, Hong HS, Choi SY. Three-dimensional contrast-enhanced hepatic MR imaging: comparison between a centric technique and a linear approach with partial Fourier along both slice and phase directions. J Magn Reson Imaging 2011;33(1):160–166.

Biomarkers, 2013; 18(1): 82–87
© 2013 Informa UK, Ltd.
ISSN 1354-750X print/ISSN 1366-5804 online
DOI: 10.3109/1354750X.2012.738249

informa
healthcare

RESEARCH ARTICLE

Higher hepatic gene expression and serum levels of matrix metalloproteinase-2 are associated with steatohepatitis in non-alcoholic fatty liver diseases

Hidenori Toyoda[1], Takashi Kumada[1], Seiki Kiriyama[1], Makoto Tanikawa[1], Yasuhiro Hisanaga[1], Akira Kanamori[1], Toshifumi Tada[1], and Yoshiki Murakami[2]

[1]*Department of Gastroenterology, Ogaki Municipal Hospital, Ogaki, Japan and* [2]*Center for Genomic Medicine, Kyoto University Graduate School of Medicine, Kyoto, Japan*

Abstract

We investigated the gene expression of tissue inhibitor metalloproteinases (TIMPs) and matrix metalloproteinases (MMPs) and serum levels of TIMPs, MMPs, and hyaluronic acid that are associated with liver fibrosis in 64 patients with nonalcoholic fatty liver diseases (NAFLD). Whereas, no differences were found between patients with and without nonalcoholic steatohepatitis (NASH) in serum levels of hyaluronic acid when excluding NASH patients with advanced fibrosis, the quantity of MMP2 mRNA in liver tissue and serum MMP2 levels were significantly higher in patients with NASH than those without, even focusing on patients with less advanced fibrosis, indicating the initiation of liver fibrosis.

Keywords: Non-alcoholic fatty liver disease, non-alcoholic steatohepatitis, matrix metalloproteinases, tissue inhibitors of metalloproteinases, hyaluronic acid, gene expression, serum levels

Introduction

Nonalcoholic fatty liver disease (NAFLD) is one of the most common liver diseases in both Western and Asian countries (Angulo 2002; Clark et al. 2003; Kojima et al. 2003; Chitturi et al. 2007; Torres & Harrison 2008), affecting 30% of the general Western adult population (Musso et al. 2010). NAFLD encompasses a histological spectrum that ranges from simple steatosis to nonalcoholic steatohepatitis (NASH). Whereas simple steatosis is usually benign, patients with NASH can progress to cirrhosis and end-stage liver disease (Angulo 2002; Fassio et al. 2004; Hashimoto et al. 2005). Therefore, it is important to differentiate patients with NASH from patients with more benign forms of NAFLD.

Liver fibrosis accumulates with the progression of NASH toward cirrhosis, as is reported in the case of viral hepatitis. Changes in many proteins associated with fibrosis have been reported during the course of viral hepatitis. Matrix metalloproteinases (MMPs) and their inhibitors (tissue inhibitors of metalloproteinases, TIMPs) are reportedly associated with the progression of liver fibrosis (Hemmann et al. 2007). It is unclear whether changes in the gene expression of fibrosis-associated proteins occur in the liver of patients with NASH, as they do in patients with viral hepatitis, and whether there are differences in the gene expression patterns and serum levels of these proteins between NASH and simple steatosis. In the present study, we investigated the gene expression patterns of several fibrosis-associated proteins in the livers of patients with NAFLD, comparing patients with and without NASH. Serum levels of fibrosis-associated proteins were also investigated.

Patients and methods

Patients

The study population consisted of 64 patients (36 males and 28 females with a mean age of 51.0 ± 15.0

Address for Correspondence: Hidenori Toyoda, MD, PhD, Department of Gastroenterology, Ogaki Municipal Hospital, 4–86, Minaminokawa, Ogaki, Gifu, 503–8502, Japan. Tel: +81-584-81-3341. Fax: +81-584-75-5715. E-mail: tkumada@he.mirai.ne.jp

(Received 13 August 2012; revised 24 September 2012; accepted 05 October 2012)